

Quantum Chemical Studies for Inhibitory Action of 3-hydroxybenzo [d] Isoxazole Tautomers on Steel and Thermodynamic, Non-linear Optical Properties (NLO) using of Density Functional Theory Method (DFT)

By

Ashutosh Kumar, Anjali Pandey and Anil Mishra

ISSN 2319-3077 Online/Electronic

ISSN 0970-4973 Print

UGC Approved Journal No. 62923

MCI Validated Journal

Index Copernicus International Value

IC Value of Journal 82.43 Poland, Europe (2016)

Journal Impact Factor: 4.275

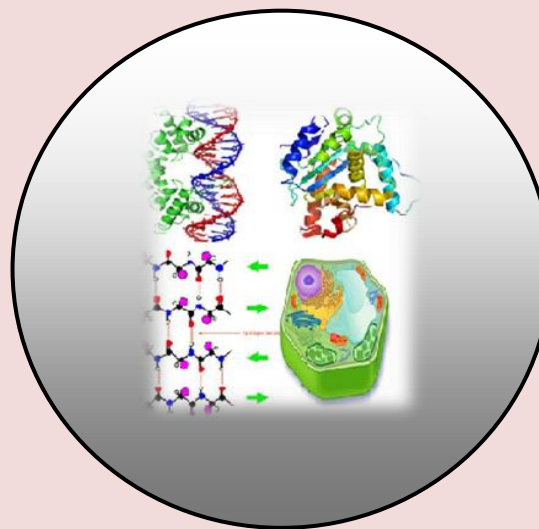
Global Impact factor of Journal: 0.876

Scientific Journals Impact Factor: 3.285

InfoBase Impact Factor: 3.66

J. Biol. Chem. Research

Volume 36 (1) 2019 Pages No. 1-13



Journal of Biological and Chemical Research

An International Peer Reviewed / Referred Journal of Life Sciences and Chemistry

Indexed, Abstracted and Cited: Index Copernicus International (Europe), Validated Medical Council of India, World Science Index, Polish Ministry of Science and Higher Education (Poland, Europe) Research Bible (Japan), Scientific Journals Impact Factor Master List, Directory of Research Journals Indexing (DRJI), Indian Science. In, Database Electronic Journals Library (Germany), Open J-Gate, J Gate e-Journal Portal, Info Base Index, International Impact Factor Services (IIFS) (Singapore), Scientific Indexing Services (USA), International Institute of Organized Research (I2OR), Cosmos Science Foundation (Germany), Science Library Index (UAE), Eye Source, Swedish Scientific Publication, World Cat, International Innovative Journal Impact Factor, Einstein Institute for Scientific Information {EISI} and Impact Factor.pl - Kompendium wiedzy o czasopismach naukowych, Philadelphia citefactor.org journals indexing Directory Indexing of International Research Journals

Published by Society for Advancement of Sciences®



Ashutosh Kumar

[http:// www.sasjournals.com](http://www.sasjournals.com)

[http:// www.jbcr.co.in](http://www.jbcr.co.in)

jbicrchemres@gmail.com

RESEARCH PAPER

Received: 06/12/2018

Revised: 15/01/2019

Accepted: 16/01/2019

Quantum Chemical Studies for Inhibitory Action of 3-hydroxy-benzo [d] Isoxazole Tautomers on Steel and Thermodynamic, Non-linear Optical Properties (NLO) using of Density Functional Theory Method (DFT)

Ashutosh Kumar, Anjali Pandey and Anil Mishra

Department of Chemistry, Faculty of Science, Central Facility for Computational Research (CFCR)
(Computer Cluster), University of Lucknow, Lucknow- 226007, India

ABSTRACT

In the present work, we have theoretically studied the inhibitory activity of keto-enol tautomers of 3-keto-benzo [d] isoxazole namely benzo [d] isoxazole-3-(2H)-one (M1) and benzo [d] isoxazole-3-ol or 3-hydroxy-benzo [d] isoxazole (M2) has been performed using density functional theory (DFT) B3LYP, CAM-B3LYP// 6-311 ++ G (2d, 2p) basis set level in order to investigate the different inhibition efficiencies of these compounds as corrosion inhibitors. The calculated structural parameters correlated to the inhibition efficiencies are the frontier molecular orbital energies E_{HOMO} (Highest occupied molecular orbital energy), E_{LUMO} (Lowest unoccupied molecular orbital energy), energy gap(ΔE), dipole moment (μ), hardness (η), softness (S), the absolute electronegativity (χ), the electrophilicity index(ω), polarizability (α), first static hyperpolarizability (β_{tot}) and the fraction of electron transferred (ΔN) from keto-enol tautomer molecule to iron (Fe). The highest value of E_{HOMO} is -6.74308357 eV calculate at B3LYP/6-311++G (2d, 2p) level and -8.19144 eV at CAM-B3LYP/6-311++G (2d, 2p) level of M1 indicates the better inhibition efficiency than the other inhibitor M2. In our study, the trend for the (ΔE_g gap) values follows the order $M1 > M2$, which suggest that inhibitor M1 has the highest reactivity in comparison to M2 and would therefore likely interact strongly with the metal surface. The parameters like hardness, softness, dipole moment, electron affinity, ionization potential, electronegativity and the fraction of electron transferred(ΔN) confirms the inhibition efficiency in the order of $M1 > M2$. We have also studied the Milliken population analysis and non-linear optical property of tautomers.

Keywords - 3-Hydroxy-Benzo [d] Isoxazol, Keto-Enol Tautomers, Molecular Descriptors, HOMO- LUMO energies, DFT Method and NLO Properties.

INTRODUCTION

Heterocyclic compounds that containing benzene fused isoxazole ring structure exhibit wide range of biological property (A.M. Katritzky, et.al. 2009, J. Clayden, et. al. 2001). The functionalized benzo [d] isoxazole have variety of uses, including pharmaceutical drugs such as some antipsychotics (including risperidone, paliperidone,

ocaperidone and iloperidone) (A.K. Jain, et. al. 1988) and the anticonvulsant zonisamide. A benzo[d]isoxazole derivative exists in keto and enol tautomeric forms (Figure 1) and consequently acts as ambidentate ligand.



Figure 1. The tautomeric forms of Benzo [d] isoxazole derivatives.

The phenomenon of corrosion of materials has been very important and challenging topic for scientist and researchers for a long time due to its varying effects on industries equipments like mining equipments, reaction vessels engineering vehicles and packaging machineries. The contamination of industrial products by corrosion is the major challenge (Y. Furukawa, et. al.2002). Corrosion also involves the deterioration of metal which is widely common in metal although it is not limited to them. Different type of materials such as plastic, ceramics and composites are also prone to the wrath of corrosion. Effects of corrosion are very harmful to all human beings, animals and whole environment. These effects not only damage the economy of any country but also leave negative impact on human health. The importance of studying steel corrosion is related to the fact that various iron metals have several industrial applications. The exposure of iron metals to harsh conditions, such as low and high pH environments usually found in petroleum or chemical industries mar lead to corrosion of these metals, thereby losing their mechanical properties. This loss causes metals to compromise on their optimum performance. Quantum chemical methods have been very useful to be determining the molecular structure as well as elucidating the electronic structure and reactivity (E. Kraka, et. al. 2000). Herein a common practice to carry out quantum chemical calculation in corrosion inhibition studies. The concept of evaluation the efficiency of corrosion inhibitor with the help of computational chemistry is to search for compounds requisite properties using chemical intuition and experience into a mathematically quantified and computerized form. Once a correlation between the molecular structure, reactivity and activity or property is found, any number of compounds, including those not yet synthesized, can be readily screened employing computational methodology (M. Karelson, et. al. 1996). The study of corrosion inhibition and processes by organic inhibitors is a very active and interesting field of research (M. Bouayed, et. al. 1999). Many scientist and researchers report that inhibition effect mainly depends on the some electronic and physiochemical properties of the organic inhibitor which relate to its electronegative functional groups, electronic density of donor atoms, steric effects, orbital character of donating electrons (M.A. Quraishi, et. al. 2002, E. Stupnisek-Lisac, et.al.1994) and π -electrons in triple or conjugated double bonds, and so on. Organic compounds containing heteroatom such as nitrogen (N), sulphur (S), oxygen (O) and phosphorus (P) as well as aromatic rings in their structure are the major adsorption centers, act as a good inhibitor (M. Hosseini, et. al. 2003, N.C. Subramanyam, et. al. 1993). Corrosion inhibitors facilitate in the retardation of metal corrosion through the formation of adsorption film between metal surface and the compound of interest. The mechanism of formation of these adsorption films may be classified as physisorption, chemisorption or a combination of the two, that is, mixed type. Physisorption or physical adsorption associated with the electrostatic interactions between charged metal and charged molecules while chemisorption or chemical adsorption associated with the formation of covalent bond resulting from the charge sharing or transfer from corrosion inhibitor molecules to metal surface (I.B. Obot, et. al. 2011). The strength and stability of the formed adsorption layer depends entirely on type of metal, the nature of the corrosion inhibitor, the type of interaction that exist between the d-orbital of the iron (Fe) metal and the π -orbital of the corrosion inhibitor, corrosive effects and the nature of corrosive medium (G. Avci 2008).

Recently, theoretical investigations of the efficiency of corrosion inhibitors has become very popular in parallel with the progress in computational chemistry and the development of efficient algorithms which assisted the routine development of molecular quantum chemical calculations (A. Domenicano, et.al. 1992). Due to the very complex type of studies which need to consider the inhibitor, metallic surface and solvent molecules, theoretical investigations of the corrosion inhibitor processes cannot be achieved in a simple way from the viewpoint of quantum chemistry.

COMPUTATIONAL DETAILS

All the geometries of tautomers have been fully optimized using the B3LYP and CAM-B3LYP method within the framework of density functional theory (DFT) in conjunction with the 6-311++G (2d, 2p) basis set i.e., Becke's three parameters non-local hybrid exchange potential with the non-local correlation functional of Lee, Yang and Parr (B3LYP) (A.D. Becke (1993, C. Lee, et.al. 1988), coulomb-attenuating method-B3LYP (CAM-B3LYP) predicts energetic quantities to the accuracy of B3LYP, while for charge transfer energies it is possible to achieve chemical accuracy (0.1eV). This functional is hybrid functional with improved long- range properties (T. Yanai, et. al. 2004). Following the geometry optimization, analytical frequency calculations were proceeded at the DFT/6-311++G (2d, 2p) level, using the following standard procedures, to obtain the thermochemical properties. All these calculation were carried out on an Intel (R) core (TM) i3-2370M CPU @ 2.40GHz, personal computer by means of GAUSSIAN 09 program package (M.J. Frisch, et. al. 2009). These calculations have been widely used to study the reaction mechanism (Z. Tao, et. al. 2010). These tools are also proved to be very useful for the study of the inhibition of the corrosion of metals (K.C. Emregul, et.al. 2006, K.F. Khaled, et.al. 2005). Recently, DFT has been to analyze the characteristics of the inhibitor/ surface mechanism and to describe the structural nature of the inhibitor in the corrosion process (M. Lashkari, et.al. 2004).

GLOBAL AND LOCAL REACTIVITY DESCRIPTORS

CHEMICAL REACTIVITY

The chemical reactivity descriptors calculated using density functional theory (DFT): total energy (E), the chemical potential (μ), chemical hardness (η), softness (S) and electrophilicity index (ω). The basic relationship of the density functional theory of chemical reactivity is precise, the one established by Parr, Donnelly, Levy and Palke (R.G. Parr, et.al. 1978), that links the chemical potential of density functional theory (DFT) with the first derivative of the energy with respect to the number of electrons, and therefore with the negative of the electronegativity (χ).

$$\chi = -\mu \left(\frac{\partial E}{\partial N} \right)_{v(r)} \quad (1)$$

Where μ is the chemical potential, E is the total energy, N is the number of electrons, and $v(r)$ is the external potential of the system. Hardness (η) has been defined within the density functional theory (DFT) as the second derivative of the E with respect to N as (v_r) property which measures both the stability and reactivity of the molecule (R.G. Parr, et.al. 1983).

$$\eta = \frac{1}{2} \left(\frac{\partial^2 E}{\partial N^2} \right)_{v(r)} \quad (2)$$

Where μ and $v(r)$ are the electronic chemical and external potentials respectively.

According to, the Koopman's theorem (T. Koopmans, 1993) for closed shell molecules, ionization potential (IP) and electron affinity (EA) can be expressed as follows in terms of E_{HOMO} and E_{LUMO} , the HOMO (highest occupied molecular orbital) energy, and the LUMO (lowest unoccupied molecular orbital) energy, respectively:

$$\text{IP} = -E_{\text{HOMO}} \text{ and } \text{EA} = -E_{\text{LUMO}} \quad (3)$$

When the values of IP and EA known, one can determine through the following expressions (R.G. Pearson, 1963) the values of the absolute electronegativity (χ), the absolute hardness (η) and softness (S):

$$\chi = I + A / 2 \text{ and } \eta = I - A / 2 \quad (4)$$

The global softness (S) is the inverse of the global hardness (η) (R.G. Parr, et. al. 1999):

$$S = 1/\eta \quad (5)$$

The electrophilicity is a global descriptor of reactivity that permits a quantitative classification of the global electrophilic nature of a molecule within a relative scale. Parr has proposed the electrophilicity index as a measure of energy lowering due to maximal electron flow between donor and acceptor and defined electrophilicity index (ω) (P.W. Ayers, et.al. 2005) as follows:

$$\omega = \mu^2 / 2 \eta \quad (6)$$

Moreover, for a reaction of two systems with different electronegativity, the electronic flow will occur from the molecule with the lower electronegativity (the organic inhibitor) towards that of higher value (the metallic surface), till the chemical potential are equal (K.F. Khaled, 2010). Therefore the fraction of electron transferred (ΔN) from the inhibitor molecule to the metallic atom was calculated according to the Pearson electronegativity scale (K.F. Khaled, 2010):

$$\Delta N = \chi_{\text{Fe}} - \chi_{\text{inh}} / 2 (\eta_{\text{Fe}} + \eta_{\text{inh}}) \quad (7)$$

Where χ_{Fe} and χ_{inh} denote the absolute electro-negativity of Fe and the inhibitor molecule, respectively; η_{Fe} and η_{inh} denote the absolute hardness of Fe and the inhibitor molecule, respectively. A theoretical value for the electro-negativity of bulk iron was used $\chi_{\text{Fe}} = 7$ eV and a global hardness of $\eta_{\text{Fe}} = 0$, by assuming that for a metallic bulk ionization potential (IP) = (EA) electron affinity because they are softer than the neutral metallic atoms (V.S. Sastri, et. al. 1997).

According to Gomez et al., the simple charge transfer model for donation and back-donation of charges between metal to inhibitor molecule proposed recently (B. Gomez, et. al. 2006). An electronic back-donation process might be occurring lead the interaction between the inhibitor molecule and the metal surface (steel). The idea initiates that if both processes occur, namely charge transfer to the molecule and back-donation from the molecule, the energy change is directly related to the hardness of the molecule, as indicated in the following expression.

$$\Delta E_{\text{Back-donation}} = - \eta / 4 \quad (8)$$

The ($\Delta E_{\text{Back-donation}}$) implies that when $\eta > 0$ and $\Delta E_{\text{Back-donation}} < 0$ the charge transfer to a molecule, followed by a back-donation from the molecule, is energetically favored. In this context, hence, it is possible to compare the stabilization among inhibiting molecules, since there will decrease as the hardness increases.

RESULTS AND DISCUSSIONS

MOLECULAR GEOMETRY PROPERTIES

The geometries for keto and enol forms of benzo [d] isoxazole molecule were fully optimized at DFT level of theory using a B3LYP and CAM-B3LYP functional together with 6-311++G (2d, 2p) basis set in gaseous phase and the absence of imaginary frequencies in the vibrational spectrum proves that the equilibrium structures correspond to the minimal energy for each tautomer. The final optimized geometries are given in Figure 2 Table 1 represents the bond lengths and their angle measurement.

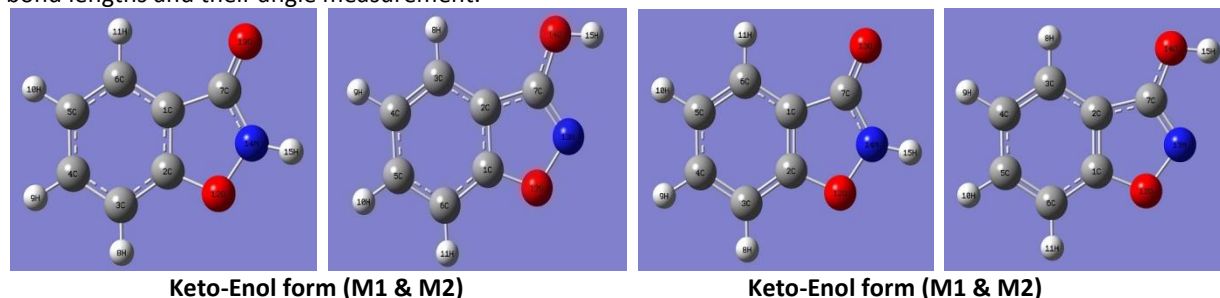


Figure 2. The optimized geometries for keto (M1) and enol (M2) form of benzo [d] isoxazole molecule at B3LYP/6-311++G (2d, 2p) and CAM-B3LYP/6-311++G (2d, 2p) level.

From **table 1** comparing bond angle and lengths of B3LYP with those of CAM-B3LYP level at 6-311++G (2d, 2p) basis set. According to the molecular structure of tautomeric form have mainly six different bonds lengths between different atoms such as C-C, C-N, C-O, O-H, O-N, and N-H. The bond lengths between C4-C5 in the benzene ring are higher value for comparing to other C-C bonds in benzene ring due to the fusion of isoxazole moiety at these carbons of both tautomeric forms. The C1-O12 bond length of M2 is 1.3479 and 1.3543 Å and C2-O12 bond length of M1 is 1.3663 and 1.3701 at CAM-B3LYP and B3LYP level of 6-311++G (2d, 2p) basis set. The C7-O14 bond length of M2 is 1.3367 and 1.3431, longer than C7-O13 bond length is 1.2103 and 1.2158 Å. The C7-N13 bond length of M2 is 1.2912 and 1.3003 Å is shorter than keto form M1 bond length 1.3726 and 1.3809 is longer.

Table 1. Results of DFT/B3LYP/6-311++G (2d, 2p) and DFT/CAM-B3LYP/6-311++G (2d, 2p) calculations on bond distance (Å), bond angle (°) and some selected dihedral angles (°) of keto – Enol tautomer in vacuum.

Benzo[d]isoxazol-3-ol (M2)			Benzo[d]isoxazol-3(2H)-one (M1)		
Methods →	CAM-B3LYP//6-311++G(2d, 2p)	B3LYP//6-311++G(2d, 2p)	CAM-B3LYP//6-311++G(2d, 2p)	B3LYP//6-311++G(2d, 2p)	
Bond	Å	Å	Bond	Å	Å
C1-C2	1.3844	1.3935	C1-C2	1.3793	1.3872
C1-C6	1.3868	1.3904	C1-C6	1.3864	1.3917
C1-O12	1.3479	1.3543	C1-C7	1.4695	1.4728
C2-C3	1.3924	1.3972	C2-C3	1.3823	1.3867
C2-C7	1.4305	1.4323	C2-O12	1.3633	1.3701
C3-C4	1.3771	1.3842	C3-C4	1.3824	1.3894
C3-H8	1.0798	1.0803	C3-H8	1.0791	1.0797
C4-C5	1.4035	1.4074	C4-C5	1.3989	1.4034
C4-H9	1.0799	1.0806	C4-H9	1.0806	1.0813
C5-C6	1.379	1.3868	C5-C6	1.3803	1.3870
C5-H10	1.0807	1.0813	C5-H10	1.0798	1.0805
C6-H11	1.079	1.0797	C6-H11	1.0801	1.0806
C7-N13	1.2912	1.3003	C7-O13	1.2103	1.2158
C7-O14	1.3367	1.3431	C7-N14	1.3726	1.3809
O12-N13	1.4027	1.4178	O12-N14	1.3949	1.4060
O14-H15	0.9645	0.9660	N14-H15	1.0032	1.0042
Bond angle	(°)	(°)	Bond angle	(°)	(°)
C2-C1-C6	122.6837	122.6942	C2-C1-C6	120.4497	120.2886
C2-C1-O12	110.4366	110.4506	C2-C1-C7	107.0072	107.2174
C6-C1-O12	126.8797	126.8552	C6-C1-C7	132.5431	132.494
C1-C2-C3	120.7384	120.6224	C1-C2-C3	122.998	123.0747
C1-C2-C7	102.3171	102.4412	C1-C2-O12	112.0645	112.0843
C3-C2-C7	136.9438	136.9364	C3-C2-O12	124.9375	124.841
C2-C3-C4	117.4223	117.476	C2-C3-C4	116.0379	116.0684
C2-C3-H8	121.052	121.0592	C2-C3-H8	121.7118	121.7724
C4-C3-H8	121.5257	121.4648	C4-C3-H8	122.2503	122.1592
C3-C4-C5	121.013	121.0602	C3-C4-C5	121.9945	121.9267
C3-C4-H9	119.8241	119.7743	C3-C4-H9	118.911	118.8914
C5-C4-H9	119.163	119.1654	C5-C4-H9	119.0945	119.182
C4-C5-C6	122.0628	121.9979	C4-C5-C6	120.6443	120.6941
C4-C5-H10	118.9065	118.9697	C4-C5-H10	119.3433	119.3486
C6-C5-H10	119.0307	119.0324	C6-C5-H10	120.0124	119.9572
C1-C6-C5	116.0799	116.1492	C1-C6-C5	117.8756	117.9475
C1-C6-H11	121.6347	121.6486	C1-C6-H11	120.2100	120.2285
C5-C6-H11	122.2855	122.2022	C5-C6-H11	121.9144	121.824
C2-C7-N13	112.4521	112.741	C1-C7-O13	131.9493	132.159
C2-C7-O14	124.9628	124.8685	C1-C7-N14	102.6207	102.5661
N13-C7-O14	122.5851	122.3905	O13-C7-N14	125.4299	125.2749
C1-O12-N13	107.9428	107.8606	C2-O12-N14	103.9609	103.7541
C7-N13-O12	106.8508	106.5066	C7-N14-O12	114.3466	114.3781
C7-O14-H15	108.7721	108.5777	C7-N14-H15	130.4633	130.8182
			O12-N14-H15	115.1901	114.8087
Dihedral angle	(°)	(°)	Dihedral angle	(°)	(°)
C2-C7-N13-O12	0.0143	0.0132	C1-C7-N14-O12	0.0422	-0.0165
O14-C7-N13-	-179.9893	180.0092	C1-C7-N14-H15	-179.9551	-180.0088

O12					
C2-C7-O14-H15	-180.0037	-180.0042	O13-C7-N14-O12	179.9635	180.0113
N13-C7-O14-H15	0.0003	0.0003	O13-C7-N14-H15	-0.0338	0.019
C1-O12-N13-C7	-0.0134	-0.0123	C2-O12-N14-C7	-0.0268	0.0108
			C2-O12-N14-H15	179.9709	180.0043

It is observed that in M1 molecule bond angle at the point of substitution C1-C2-C3 is 122.998 and 123.0743 in degree ($^{\circ}$) and M2 molecule bond angle is shorter i.e. 120.7384 and 120.6224 in degree ($^{\circ}$) in CAM-B3LYP and B3LYP level respectively. The bond angle C1-C7-O13 of M1 is longer (131.9493 and 132.1590 in degree ($^{\circ}$)) than the C2-C7-O14 of M2 (124.9628 and 124.8685) of the same level. The variation in bond angle depends on the electronegativity of the central atom, the presence of lone-pair of electrons and the conjugation of double bonds. If the electronegativity of the central atom is less, the bond angle is decreased.

ELECTRONIC PROPERTIES

According to frontier molecular orbital theory (FMO) of chemical reactivity, the transition of an electron is due to the interaction between highest occupied molecular orbital (HOMO) and lowest unoccupied molecular orbital (LUMO) of reacting species (P. Udhayakala, et.al. 2012). Table- 2 represents the quantum chemical parameters for inhibitors M1 and M2.

Table 2. Global chemical reactivity indices for M1 and M2 calculated using B3LYP/6-311++G (2d, 2p) and CAM-B3LYP/6-311++G (2d, 2p) level in vacuum.

Electronic properties	B3LYP/6-311++G (2d, 2p)		CAM-B3LYP/6-311++G (2d, 2p)	
	Keto form (M1)	Enol form (M2)	Keto form (M1)	Enol form (M2)
Energy (a.u.)	-475.05336924	-475.05471421	-474.83280983	-474.83419988
HOMO (eV)	-6.74308357	-6.86362697	-8.19123702	-8.295454
LUMO (eV)	-1.61005712	-1.53332294	-0.35156224	-0.26775329
I (eV)	6.74308357	6.86362697	8.19123702	8.295454
A (eV)	1.61005712	1.53332294	0.35156224	0.26775329
ΔE_{gap} (eV)	5.13302645	5.33029757	7.833967478	8.02770071
χ (eV)	4.17657034	4.19847496	4.27139961	4.28160364
η (eV)	2.56651322	2.66515202	3.91983739	4.01385036
μ (eV)	-4.17657034	-4.19847496	-4.27139961	-4.28160364
S (eV $^{-1}$)	0.3896336324576	0.375213118	0.25511262	0.24913734
ω (eV)	3.3983343	3.30697684	2.32724636	2.28360901
ΔN	0.550051649	0.525584473	0.3480502	0.33862702
$\Delta E_{\text{Back-Donation}}$ (eV)	-0.641628305	-0.666288005	-0.97995935	-1.00346259
μ (D)	3.5525	2.0898	3.5849	2.1291
ΔN_{Max}	1.62733249	1.57532288	1.08968796	1.06670734

The energy of HOMO measures the tendency towards the donation of an electron by a molecule. Therefore, the higher value of E_{HOMO} indicates a better tendency towards the donation of the electron, enhancing the adsorption of the inhibitor on mild steel and therefore better inhibition efficiency. E_{LUMO} (energy of lowest unoccupied molecular orbital) shows the capacity of the molecule to accept electrons. The binding capacity of the inhibitor to the metal surface increases with increasing of the HOMO (highest occupied molecular orbital) and decreasing of the LUMO energy values. FMO diagrams of M1 and M2 is represented in **figure-3**.

The energy of the HOMO (E_{HOMO}) provides information about the electron donating property of the molecule. The molecule with the highest E_{HOMO} value often has the highest tendency to donate electrons to an appropriate acceptor molecule of low empty molecular orbital energy (G. Gece, et. al. 2009).

The inhibitor does not only donate an electron to the unoccupied d-orbital of the metal leading to the formation of a feedback bond. The highest value of E_{HOMO} is -6.74308357 eV and -8.19123702 eV of M1 at B3LYP/6-311++G (2d, 2p) and CAM-B3LYP/6-311++G (2d, 2p) level respectively; indicate the better inhibition efficiency than the other inhibitor M2.

The energy gap between the highest occupied molecular orbital (HOMO) and the lowest unoccupied molecular orbital (LUMO) (ΔE) provides information about the overall reactivity of a molecule. As ΔE_{Gap} decreases, the reactivity of molecule increases leading to an increase in the inhibition efficiency of the molecule (M.K. Awad, et.al. 2010). The low value of the ($\Delta E = E_{\text{LUMO}} - E_{\text{HOMO}}$) gap will render good inhibition efficiencies since the energy to remove an electron from the last occupied orbital will be minimized (O. Chris, et. al. 2012). A molecule or compound with a low energy gap (ΔE_{gap}) is more polarizable and is generally related with high chemical activity and low kinetic stability and is called soft molecule (I. Fleming, 1976). In our study, the trend for the (ΔE_{gap}) values follows the order $M1 > M2$ at both levels of the DFT calculation, which suggests that inhibitor M1 has the highest reactivity in contrast to the compound M2 and would therefore likely interact strongly with the metal surface.

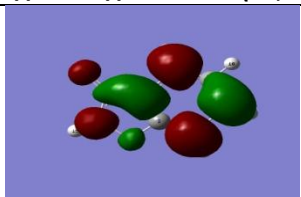
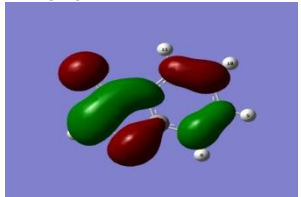
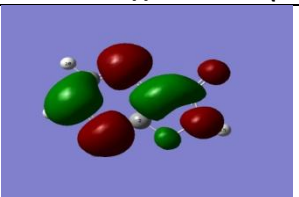
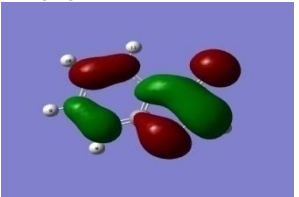
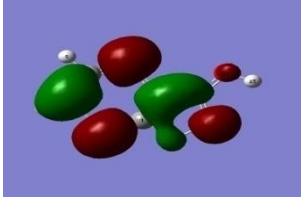
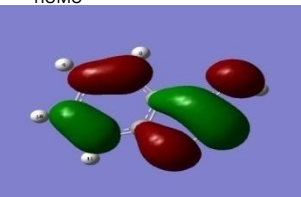
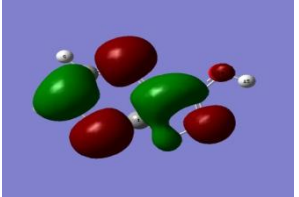
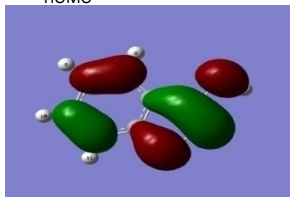
Tautomeric form	DFT//B3LYP//6-311++G (2d, 2p)	DFT//CAM-B3LYP//6-311++G (2d, 2p)
Keto - form (M1)	 <p> $E_{\text{LUMO}} = -1.61005712$ eV $\Delta E_{\text{Gap}} = 5.13302645$ eV $E_{\text{HOMO}} = -6.74308357$ eV </p> 	 <p> $E_{\text{LUMO}} = -0.35156224$ eV $\Delta E_{\text{Gap}} = 7.833967478$ eV $E_{\text{HOMO}} = -8.19123702$ eV </p> 
Enol - form (M2)	 <p> $E_{\text{LUMO}} = -1.53332294$ eV $\Delta E_{\text{Gap}} = 5.33029757$ eV $E_{\text{HOMO}} = -6.86362697$ eV </p> 	 <p> $E_{\text{LUMO}} = -0.26775329$ eV $\Delta E_{\text{Gap}} = 8.02770071$ eV $E_{\text{HOMO}} = -8.295454$ eV </p> 

Figure 3. Frontier molecular orbital (FMO) diagrams of M1 and M2 by B3LYP/6-311++G (2d, 2p) and CAM-B3LYP/6-311G (2d, 2p).

The important global chemical reactivity parameters summarized in table 2. Ionization energy is a basic descriptor of the chemical reactivity of compounds. High ionization energy shows high stability and chemical inertness and small ionization energy shows high reactivity of the compounds (T. Chakraborty, et. al. 2010). The low ionization energy 6.74308357 eV and 8.19123702 eV of M1 at B3LYP/6-311++G (2d, 2p) and CAM-B3LYP/6-311++G (2d, 2p) level of the DFT calculation indicate the high inhibition efficiency.

Total hardness (η) and softness (S) are main properties to measure the molecular stability and reactivity. It is noticeable that the chemical hardness (η) basically denotes the resistance towards the distortion or polarization of the electron cloud of the atoms, ions or molecules under a small perturbation of chemical reaction. A hard molecules or compounds have a large energy gap (ΔE) and a soft molecule has a small energy gap (ΔE) (N.O. Obi-Egbedi, et. al. 2011). In our present study, M1 with low hardness value, 2.56651322 eV and 3.91983739 eV calculated at B3LYP and CAM-B3LYP level, compared with other compound have a low energy gap. Commonly the inhibitor with the least value of global hardness (η) (hence the highest value of global softness) is predicted to have the highest inhibition capability (E.E. Ebenso, et. al. 2010). For the transfer of electron, adsorption could occur at the part of the molecule where softness (S), which is a local property, has a highest value (R. Hasanov, et. al. 2007). M1 with the softness value of 0.3896336324576 eV (B3LYP) and 0.25511262 eV (CAM-B3LYP) has the highest inhibition efficiency

Table-2 shows the order of electronegativity as $M2 > M1$. Consequently, an increase in the variance of electronegativity between the metal and the inhibitor is detected in the order $M1 > M2$. As stated by Sanderson's electronegativity equalization principle (P. Geerlings, et. al. 2002), M2 with a high electronegativity and low variance of electronegativity quickly reaches equalization and hence low reactivity is expected which in turn shows low inhibition efficiency. The ΔN (number of electrons transferred) and $\Delta E_{\text{Back-donation}}$ was also calculated and tabulated in **Table-2**. Values of number of electrons transferred (ΔN) shows that the inhibition efficiency resulting from electron donation sympathizes with Lukovits's work (I. Lukovits, et. al. 2001). If number of electrons transferred (ΔN) < 3.6 , the inhibition efficiency increases by increasing electron -donating ability of these inhibitors to donate electrons to the metal surface and it increases in the following order: $M1 > M2$. Thus, the highest fraction of electrons transferred is associated with the best inhibitor (M1), while the least fraction is associated with the inhibitor that has the least inhibition efficiency (M2).

THERMODYNAMIC PROPERTIES

Table-3 lists the values of total thermal energy (E), total heat capacity (Cv), total entropy (S), ΔE , ΔH , ΔG , zero-point vibrational energy and rotational constant for the tautomerization reaction: 3-KBDI \longleftrightarrow 3-HBDI computed by utilizing B3LYP and CAM-B3LYP methods with 6-311++G (2d, 2p) basis set at 298.15 K. in gas phase. The results reported in **Table-3** reveal that the relative energies of tautomer are slightly affected on going from B3LYP level to CAM-B3LYP level, which means that the inclusion of relatively higher order electron correlation has an insignificant effect on the relative stability of both tautomeric forms. However, the result shows that of M2 are greatly stabilized ongoing from B3LYP/6-311++G (2d, 2p) to CAM-B3LYP/6-311++G (2d, 2p) level. The differences in zero-point vibrational energies (ZPVEs) appear to be significant. The ZPVEs is lower by the B3LYP/6-311++G (2d, 2p) method than by the CAM-B3LYP method. The high value of ZPVE M2 is 69.80698 K.cal/mol obtained at DFT/CAM-B3LYP/ 6-311++G (2d, 2p) whereas the smallest value of M1 is 68.19690 K.cal/mol obtained at DFT/B3LYP/6-311++G (2d, 2p) level.

MULLIKEN ATOMIC CHARGES

Mulliken atomic charge calculation is an important tool in the application of quantum chemical calculation to the molecular system because atomic charges influence dipole moments, molecular polarizability, electronic structure and other physical properties of molecular systems. The calculated Mulliken atomic charges are listed in **table-4**. The atomic charge depends on basis set probably occur due to the polarization. From **table-4** the atoms show negative charges, which are donor atom and atoms shows positive charges, which are the acceptor atom. A comparison of Mulliken's atomic charge obtained by the two theoretical (B3LYP & CAM-B3LYP) approaches illustrated in **figure-4** and **figure-5**. It may be discerned that the two methods give similar atomic charges.

Table- 3. Theoretically calculated thermodynamic parameter of tautomer M1 and M2 at B3LYP/6-311++G (2d, 2p) and CAM-B3LYP/6-311++G (2d, 2p) level at 298.15 K. and 1 atm pressure in gas phase.

Parameter	DFT/B3LYP/6-311++G (2d, 2p)		DFT/CAM-B3LYP/6-311++G (2d, 2p)	
	(M1)	(M2)	(M1)	(M2)
Total E (Thermal) Kcal/Mol	72.407	73.139	73.345	74.123
Total heat capacity (Cv) (Cal/Mol-kelvin)	26.858	28.318	26.359	27.764
Total entropy (S) (Cal/Mol-kelvin)	82.170	83.019	81.808	82.606
The energy of change (ΔE) K.cal/mol	-843981452		-0.87226958	
The enthalpy of change (ΔH) K. cal/mol	-0114834238		-0.094126425	
The change of free energy (ΔG) K. cal/mol	-0.368348076		-0.332580035	
Zero point vibrational energy (k.cal/mol)	68.19690	68.75130	69.19714	69.80698
Rotational constant (GHz)	X = 2.78922 Y = 1.29053 Z = 0.88230	X = 2.82782 Y = 1.27564 Z = 0.87908	X = 2.81613 Y = 1.30133 Z = 0.89004	X = 2.85740 Y = 1.28557 Z = 0.88666

Table 4. Mulliken atomic charges of tautomer M1 and M2.

Atoms of M1	B3LYP/6-311++G (2d, 2p)	CAM-B3LYP/6-311++G (2d, 2p)	Atoms of M2	B3LYP/6-311++G (2d, 2p)	CAM-B3LYP/6-311++G (2d, 2p)
C1	0.304995	0.254560	C1	-0.373894	-0.017818
C2	0.186527	0.199354	C2	0.463248	0.243440
C3	-0.165801	-0.145067	C3	-0.549153	-0.135420
C4	0.042259	0.023453	C4	-0.018198	-0.253822
C5	-0.312426	-0.294499	C5	-0.250327	-0.024915
C6	-0.327490	-0.295810	C6	0.215486	-0.230851
C7	0.442359	0.403333	C7	0.649583	0.557506
H8	0.135807	0.140692	H8	0.135498	0.141500
H9	0.134808	0.134786	H9	0.130064	0.125972
H10	0.134380	0.127400	H10	0.131457	0.130683
H11	0.150778	0.156110	H11	0.146524	0.144364
O12	-0.261829	-0.263232	O12	-0.141865	-0.160777
O13	-0.529953	-0.528470	N13	-0.398273	-0.381095
N14	-0.143886	-0.136793	O14	-0.424698	-0.422991
H15	0.219460	0.224184	H15	0.284550	0.284243

NON LINEAR OPTICAL (NLO) ANALYSIS

Non-Linear Optical (NLO) effect is the forefront of current research because of its importance in providing the key functions of frequency shifting, optical modulation, optical switching, optical logic and optic memory for the emerging technologies in areas such as telecommunications, signal processing and optical interconnections (C. Andraud, et. al. 1994, M. Nakano, et. al. 2002, V.M. Geskin, et. al. 2003). Non-linear optics deals with the interaction of applied electromagnetic fields in various materials to generate new electromagnetic fields, altered in wave number, phase, or other physical properties. Organic molecules able to manipulate photonic signals efficiently are of importance in technologies such as optical communication, optical computing, and dynamic image processing (P.V. Kolinsky 1992, D.F. Eaton 1991).

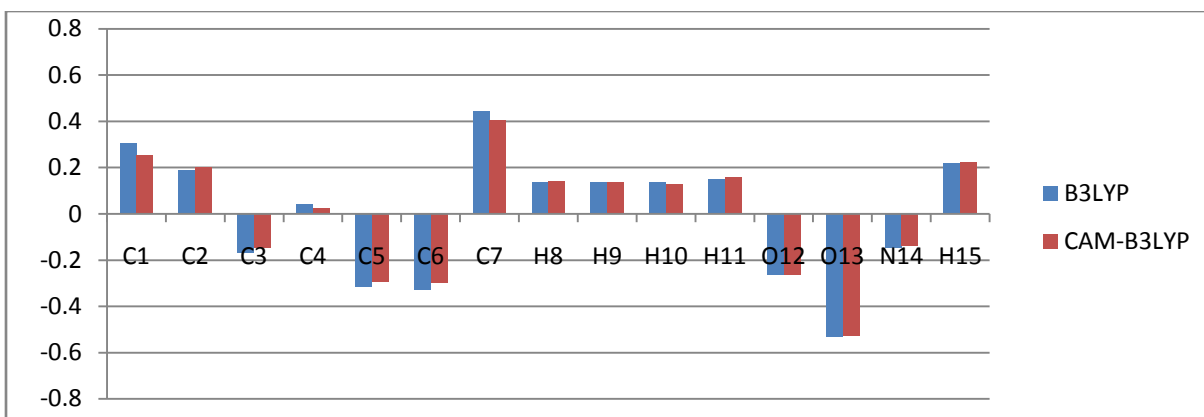


Figure 4. Mulliken's atomic charges of tautomer (M1) between theoretical (B3LYP & CAM-B3LYP) approaches.

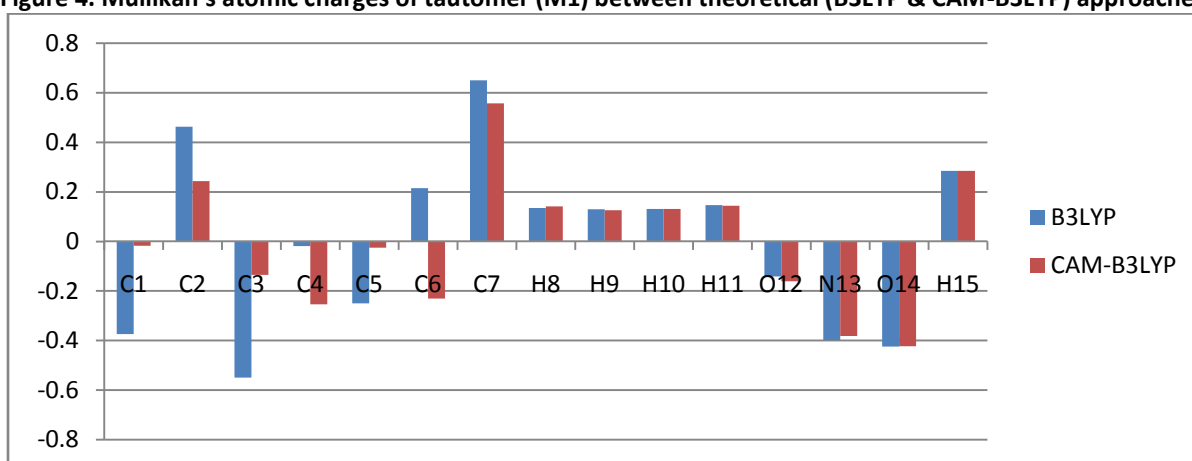


Figure 5. Mulliken's atomic charges of tautomer (M2) between theoretical (B3LYP & CAM-B3LYP) approaches.

The first static hyperpolarizability of the tautomer (M1 & M2) was calculated using the B3LYP/6-311++G (2d, 2p) and CAM-B3LYP/6-311++G (2d, 2p) basis set based on the finite field approach. The energy of a system is a function of the electric field, in the presence of an applied electric field. The first static hyperpolarizability is a third rank tensor that can be described by a 3 x 3x 3 matrix. The 27 components of the matrix can be reduced to 10 components due to Kleinman symmetry (D.A. Kleinman 1962). The complete equations for calculating the magnitude of total dipole moment μ , the average polarizability (α_{tot}) and the first hyperpolarizability β_{tot} , using the x,y,z components is as follows:

$$\mu_{tot} = (\mu_x^2 + \mu_y^2 + \mu_z^2)^{1/2} \quad (9)$$

$$\alpha_{tot} = 1/3 (\alpha_{xx} + \alpha_{yy} + \alpha_{zz}) \quad (10)$$

$$\beta_i = \beta_{iii} + 1/3 \sum (\beta_{jij} + \beta_{jji} + \beta_{jji}) \quad (11)$$

$$\beta_{tot} = \sqrt{\beta_x^2 + \beta_y^2 + \beta_z^2} \quad (12)$$

$$\langle \beta_{tot} \rangle = [(\beta_{xxx} + \beta_{xyy} + \beta_{xzz})^2 + (\beta_{yyy} + \beta_{yzz} + \beta_{yxx})^2 + (\beta_{zzz} + \beta_{zxx} + \beta_{zyy})^2]^{1/2} \quad (13)$$

Since the value of the polarizability (α_{tot}) and the hyperpolarizability (β_{tot}) of Gaussian output are reported in an atomic mass units (a.u.), the calculated values have been converted into electrostatic units (esu) (α is 1 a.u. = 0.1482×10^{-24} esu; β is 1 a.u. = $0.0086393 \times 10^{-30}$ esu). The results of electronic dipole moment μ_i (i = x, y, z), polarizability α_{ij} and first-order hyperpolarizability β_{ijk} are listed in **Table-5**. The calculated dipole moment of M1 is equal to 3.5524 D for the B3LYP level and 3.5849 D for the CAM-B3LYP level. The calculated polarizability α_{tot} of M1 is equal to 13.821×10^{-24} esu for B3LYP level and 13.456×10^{-24} for CAM-B3LYP level.

The calculated first static hyperpolarizability of M1 is 0.3567×10^{-30} esu for B3LYP level and 0.3584×10^{-30} for the CAM-B3LYP level and these values are greater (102.53 times for B3LYP level and 90.02 times for the CAM-B3LYP level) than that of the standard NLO material urea (0.13×10^{-30} esu) (M. Adant 1995). We conclude that both tautomeric compounds is an attractive object for future studies of nonlinear optical properties.

Table-5. Theoretically calculated dipole moment (μ), molecular polarizability $\langle\alpha\rangle$ and first static hyperpolarizability (β_{tot}) of tautomer M1 and M2 at B3LYP and CAM-B3LYP level in gas phase.

Dipole moment (μ_{tot}) (Debye)	B3LYP/6-311++G (2d, 2p)		CAM-B3LYP/6-311++G (2d, 2p)		First static hyperpolarizability (β_{tot}) (a.u.)	B3LYP/6-311++G (2d, 2p)		CAM-B3LYP/6-311++G (2d, 2p)	
	M1	M2	M1	M2		M1	M2	M1	M2
μ_x	2.5903	1.3571	2.6304	1.4067	β_{xxx}	4.608	-27.204	5.1045	-26.667
μ_y	-2.431	-1.589	-2.435	-1.598	β_{yyy}	-6.244	-4.273	-6.126	-4.377
μ_z	0.0000	0.000	-0.0003	0.0000	β_{zzz}	-0.003	-0.003	-0.004	-0.003
μ_{tot}	3.5524	2.089	3.5849	2.1291	β_{xyy}	9.602	12.494	9.9733	12.811
Polarizability $\langle\alpha\rangle$					β_{xxy}	-32.820	-10.476	-33.04	-10.336
α_{xx}	124.99	127.18	120.580	122.45	β_{xxz}	0.0017	-0.002	-0.013	-0.0024
α_{xy}	-1.870	-2.265	-2.105	-2.123	β_{xzz}	-9.663	-9.594	-9.697	-9.618
α_{yy}	102.83	100.68	100.600	98.666	β_{yzz}	-1.973	2.002	-1.970	2.020
α_{xz}	0.007	0.008	0.004	0.007	β_{yyz}	0.0022	0.0009	-0.004	0.0002
α_{yz}	0.006	0.002	0.004	0.002	β_{xyz}	0.0008	0.0001	-0.007	0.0002
α_{zz}	51.94	52.743	51.228	52.027	$\langle\beta_{\text{tot}}\rangle$ (esu)	0.3567×10^{-30}	1.1938×10^{-30}	0.3584×10^{-30}	1.1892×10^{-30}
$\langle\alpha\rangle(\text{esu}) \times 10^{24}$	13.821	13.862	13.456	13.493					

CONCLUSION

Quantum chemical calculations, using the Density Functional Theory method, have been performed on two benzo-fused isoxazole derivatives, namely benzo [d] isoxazole-3-(2H)-one (M1) and benzo [d] isoxazole-3-ol (M2) to investigate their geometric, electronic properties, thermodynamic, Mulliken charges and nonlinear optical property in an attempt to elucidate the reactivity. The inhibition efficiency of M1 & M2 increase with the increase in E_{HOMO} , and the decrease in energy gap (ΔE). The compound (M1) has the highest inhibition capability because it had the highest HOMO energy and ΔN values and it was most capable of offering electrons. The parameters like hardness (η), softness (S), dipole moments (μ), electron affinity (EA), ionization potential (IE), electro-negativity (χ) and the fraction of electron transferred (ΔN) confirms the inhibition efficiency in the order of $M1 > M2$. The calculated parameter like polarizability (α), dipole moment (μ) and first static hyperpolarizability (β_{tot}) are comparable with the reported values of tautomer M1 & M2, which makes this tautomeric compounds a desirable object for future studies of nonlinear optics.

ACKNOWLEDGEMENT

The authors convey their profound thanks to the Head, Department of Chemistry, Lucknow University, Lucknow, India for providing laboratory facilities and central facility for computational research.

REFERENCES

- Katritzky, A.M. and Pozharskii, A.F. (2009). Handbook of heterocyclic Chemistry (2nd Ed.). Academic Press. ISBN 0080429882.
- Clayden, J., Greeves, N., Warren, S. and Wothers, P. (2001). Organic Chemistry Oxford, Oxfordshire: Oxford University Press. ISBN 0-19-850346-6.

- Jain, A.K., Kelwala, S. and Gershon S. (1988).** Antipsychotic Drugs in Schizophrenia: Current Issues. *International Clinical Psychopharmacology* 3. 1-30.
- Furukawa Y., Kim J.W., Watkins J. and Wilkin R.T. (2002).** Formation of ferrihydrite and associated iron corrosion products in permeable reactive barriers of zero-valent iron. *Environ. Sci. Technol.* 36 (24). 5469-5675.
- Kraka, E. and Cremer, D. (2000).** Computer Design of Anticancer Drugs. *J. Am. Chem. Soc.* 122. 8245-8264.
- Karelson, M. and Lobanov V. (1996).** Quantum Chemical Descriptors in QSAR/QSPR Studies. *Chem. Rev.* 96. 1027-1043.
- Bouayed, M., Rabaa H., Srhiri A., Saillard J.Y. and Ben, B. (1999).** A experimental and theoretical study of organic corrosion inhibitors on iron in acidic medium. *Corros. Sci.* 41. 501-517.
- Quraishi, M.A. and Sardar, R. (2002).** Corrosion inhibition of mild steel in acid solutions by some aromatic oxadiazoles. *Mater. Chem. Phys.* 78. 425-431.
- Stupnisek-Lisac E., Podbrscek S., T. Soric T. (1994).** Non-toxic organic zinc corrosion inhibitors in hydrochloric acid. *J. Appl. Electrochem.* 24. 779-784.
- Hosseini, M., Mertens S.F.L., Ghorbani M. and Arshadi, M.R. (2003).** Asymmetrical Schiff bases as inhibitors of mild steel corrosion in sulphuric acid media. *Mater. Chem. Phys.* 78. 800-808.
- Subramanyam, N.C., Sheshardi B.S. and Mayanna S.A. (1993).** Thiourea and substituted thioureas as corrosion inhibitors for aluminium in sodium nitrite solution. *Corros. Sci.* 34. 563-571.
- Obot, I.B., Obi-Egbedi N.O., Umoren S.A. and Ebenso E.E. (2011).** Adsorption and kinetic studies on the inhibition potential of fluconazole for the corrosion of Al in HCl solution. *Chem. Eng. Comm.* 198. 711-725.
- Avci, G. (2008).** Corrosion inhibition of indole-3-acetic acid on mild steel in 0.5 M HCl. *Colloids Surf. A. Physicochem. Eng. Aspects* 317. 730-736.
- Domenicano A., Hargittai I. (1992).** Accurate molecular structures, their determination and importance. Oxford University Press. New York
- Becke, A.D. (1993).** Density-functional chemistry III The role of exact exchange. *J. Chem. Phys.* 8. 5648-5653.
- Lee C., Yang W., Parr R.G. (1988).** Development of the Colle-Salvetti correlation-energy formula into a functional of the electron density. *Phys. Rev. B.* 37. 785-793.
- Yanai, T., Tew D.P. and Handy N.C. (2004).** A new hybrid exchanges? Correlation functional using the Coulomb-attenuating method (CAM-B3LYP). *Chem. Phys. Lett.* 393. 51-57.
- Frisch, M.J., Trucks, G.W., Schlegel, H.B. et. al. (2009).** Gaussian 09, Rev. A.1. Gaussian Inc. Wallingford CT.
- Tao, Z., Zhang, S., Li, W. and Hou, B. (2010).** Adsorption and corrosion inhibition behavior of mild steel by one derivatives of benzoic-triazole in acidic solution. *Ind. Eng. Chem. Res.* 49. 2593-2599.
- Emregul, K.C. and Hayvali, M. (2006).** Studies on effect of a newly synthesized Schiff base compound from phenazone and vanillin on the corrosion of steel in 2 M HCl. *Corros. Sci.* 48. 797-812.
- Khaled, K.F., Babic-Samardzija, K. and Hackerman, N. (2005).** Theoretical study of the structural effects of polymethylene amines on corrosion inhibition of iron in acid solution. *Electro. Chem. Acta.* 50. 2515-2520.
- Lashkari, M. and Arshadi, M.R. (2004).** DFT studies of pyridine corrosion inhibitors in electrical double layer: solvent, substrate, and electric field effects. *Chem. J. Chem. Phys.* 299. 131-137.
- Parr, R.G., Donnelly, R.A., Levy, M. and Palke W.E. (1978).** Electronegativity- the density functional view point. *J. Chem. Phys.* 68. 3801-3807.
- Parr, R.G. and Pearson, R.G. (1983).** Absolute hardness: Companion parameter to absolute electronegativity. *J. Am. Chem. Soc.* 105. 7512-7516.
- Koopmans, T. (1993).** Ordering of wave functions and eigen-energies to the individual electrons of an atom. *Physica.* 1. 104-113.
- Pearson, R.G. (1963).** Hard and soft acids and bases. *J. Am. Chem. Soc.* 85 (22). 3533-3539.
- Parr, R.G., Szentpaly, L. and Liu, S. (1999).** Electrophilicity index. *J. Am. Chem. Soc.* 121. 1922-1924.
- Ayers, P.W., Anderson, J.S.M. and Bartolotti, L.J. (2005).** Perturbative perspectives on the chemical reaction prediction problem. *Int. J. Quantum. Chem.* 101. 520-534.
- Khaled, K.F. (2010).** Studies of iron corrosion inhibition using chemical, electrochemical and computer simulation techniques. *Electro. Chim. Acta.* 22. 6523.

- Sastri, V.S. and Perumareddi, J.R. (1997). Molecular orbital theoretical studies of some organic corrosion inhibitors. *Corrosion*. 53. 617.
- Gomez, B., Likhanova, N.V., Dominguez-Aguilar, M.A., Martinez Palou, R., Vela, A. and Gasquez, J. (2006). Quantum chemical study of the inhibitive properties of 2-pyridyl-azoles. *J. Phy. Chem. B*. 110. 8928-8934.
- Udhayakala, P., Rajendiran, T.V. and Gunasekaran, S. (2012). Theoretical study using dft calculations on inhibitory action of some pyrazole derivatives on steel. *J. Adv. Sci. Res.* 3 (3). 67-74.
- Gece, G. and Bilgic, S. (2009). Quantum chemical study of some cyclic nitrogen compounds as corrosion inhibitors of steel in NaCl media. *Corros. Sci.* 51. 1876-1878.
- Awad, M.K., Mustafa, M.R. and Abo Elnga, M.M. (2010). Computational simulation of the molecular structure of some triazoles as inhibitors for the corrosion of metal surface. *J. Mol. Struct. (Theochem)* 959. 66-74.
- Chris, O. Akalezi, Conrad K. Enenebaku and Emeka E. Oguzie. (2012). Application of aqueous extracts of coffee senna for control of mild steel corrosion in acidic environments. *Int. J. of Indus. Chem.* 3. 13-25.
- Fleming, I. (1976). *Frontier Orbitals and Organic Chemical Reactions*, (John Wiley and Sons) New York.
- Chakraborty T., Ghosh D.C. (2010). Computation of the atomic radii through the conjoint action of the effective nuclear charge and the ionization energy. *Mol. Phys.* 108 (16). 2081-2092.
- Obi-Egbedi, N.O., Obot, I.B., El-Khaiary, M.I., Umoren, S.A. and Ebenso E.E. (2011). Computational simulation and statistical analysis on the relationship between corrosion inhibition efficiency and molecular structure of some phenanthroline derivatives on mild steel surface. *Int. J. Electrochem. Sci.* 6. 5649-5675.
- Ebenso, E.E., Isabirye, D.A. and Eddy, N.O. (2010). Adsorption and Quantum Studies on the inhibition Potentials of Some Thiodemicarbazides for the Corrosion of Mild Steel in Acidic Medium. *Int. J. Mol. Sci.* 11. 2473-2498.
- Hasanov, R., Sadikglu, M. and Bilgic, S. (2007). Electrochemical and quantum chemical studies of some Schiff bases on the corrosion of steel in H₂SO₄ solution. *Appl. Surf. Sci.* 253. 3913-3921.
- Geerlings, P. and De Proft. F. (2002). Chemical reactivity as Described Quantum Chemical Methods. *Int. J. Mol. Sci.* 3. 276-309.
- Lukovits, I., Kalman, E. and Zucchi, F. (2001). Corrosion inhibitors correlation between electronic structure and efficiency. *Corrosion*. 57. 3-8.
- Andraud, C., Brotin, T., Garcia, C., Pelle, F., Goldner, P., Bigot, B. and Collet, A. (1994). Theoretical and experimental investigations of the nonlinear optical properties of vanillin, polyenovanillin, and bisvanillin derivatives. *J. Am. Chem. Soc.* 116. 2094-2102.
- Nakano, M., Fujita, H., Takahata, M. and Yamaguchi, K. (2002). Theoretical Study on Second Hyperpolarizabilities of Phenylacetylene Dendrimer: Toward an Understanding of Structure–Property Relation in NLO Responses of Fractal Antenna Dendrimers. *J. Am. Chem. Soc.* 124. 9648-9655.
- Geskin, V.M., Lambert, C. and Bredas, J.L. (2003). Origin of High Second- and Third-Order Nonlinear Optical Response in Ammonio/Borato Diphenylpolyene Zwitterions: the Remarkable Role of Polarized Aromatic Groups. *J. Am. Chem. Soc.* 125. 15651-15658.
- Kolinsky, P.V. (1992). New materials and their characterization photonic device applications. *Opt. Eng.* 31. 1676-1684.
- Eaton, D.F. (1991). Non-linear optical materials. *Science*. 25. 281-287.
- Kleinman, D.A. (1962). Non-linear dielectric polarization in optical media. *Phys. Rev.* 126. 1977-1979.
- Adant, M., Dupuis, L. and Bredas L. (1995). Ab initio study of the non-linear optical properties of urea: Electron correlation and dispersion effects. *Int. J. Quantum. Chem.* 56. 497-507.

Corresponding author: Ashutosh Kumar, Department of Chemistry, Faculty of Science, Central Facility for Computational Research (CFCR) (Computer Cluster), University of Lucknow, Lucknow- 226007, India.
Email: mishraanil101@hotmail.com, ashutosh.chemist@gmail.com, anjaliipandey270190@gmail.com
Contact: +91-9415006008, +91-9450497159